

Short communication

Application of non-resonant laser ionization mass spectrometry for a fast isotope analysis of metal microparticles

Kyuseok Song*, Yongjoon Park, Wonho Kim

Nuclear Chemistry Research Division, Korea Atomic Energy Research Institute, P.O. Box 105, Yusong, 305-600 Daejeon, Republic of Korea

Received 10 April 2006; received in revised form 25 May 2006; accepted 1 June 2006

Abstract

Isotope analysis of metal microparticles was performed by adopting a laser ionization mass spectrometry with slightly defocused ablation laser beam. The analyzed sample particles were Pb, Zn, Ni and Gd₂O₃. The sizes of particle size were 75, 50, 10, and < 10 μm, for Pb, Zn, Ni and Gd₂O₃, respectively. Sample particles were loaded onto a tantalum or zirconium sheet by using a Collodion. For large-sized particles such as Pb and Zn, a single particle was loaded on the metal sheet for a laser ablation, while several particles were loaded for particles with less than 10 μm in size due to a limitation in the particle handling technique. An isotope analysis was performed by a direct laser ionization followed by a mass analysis of the loaded samples with the Collodion using a 532 nm laser. A slight defocusing of the adopted laser provided a longer time for the experiment with a single microparticle. The isotope abundances of the adopted elements were measured and the deviation from the natural abundance was calculated as less than 5–10% depending on samples used except for the minor isotopes.

© 2006 Elsevier B.V. All rights reserved.

Keywords: Laser ionization mass spectrometry; Microparticle; Isotope analysis

1. Introduction

The isotope analyses of microparticles in environmental samples and swipe samples are important tasks for an environmental monitoring and nuclear safety. Airborne environmental particles can be easily analyzed by a particle mass spectrometry [1–4] by adopting a laser ionization of the particles while special concern is needed for an isotope analysis of swipe samples. Microparticles are normally analyzed either by adopting a chemical treatment or a digestion followed by conventional analytical methods or direct analysis methods such as a laser-ablation ICP mass spectrometry (LA-ICP-MS), SIMS (secondary ion mass spectrometry), SNMS (sputtered neutral mass spectrometry), and a fission track analysis followed by a thermal ionization mass spectrometric (TIMS) analysis. SIMS is known to be one of the most popular techniques so far for an isotope analysis of swipe samples [5–7]. SIMS, however, normally produces many more neutrals than secondary ions. Therefore, analytical techniques, such as SNMS, which utilizes sputtered neutrals, instead of secondary ions, for an ionization and mass analysis

have been developed. SIMS also bears difficulty for an isotope analysis of particles containing a mixture of elements due to an isobaric interference. Edermann et al. reported on a resonant and non-resonant laser ionization of sputtered uranium for the sensitive isotope analysis of swipe samples [8] and they showed an improved detection sensitivity and selectivity for the isotope analysis. They also suggested that informations about main components as well as specific isotopic information of a trace element could be obtained from the same single particle by using resonance as well as non-resonant ionization combined in a single step. The SNMS can enhance the detection sensitivity by adopting a resonance ionization while laser systems in addition to the ion beam generator are needed. Fission track analysis (FTA) or FTA followed by TIMS measurement has been also used for a single particle analysis of swipe samples [6,9,10]. LA-ICP-TOF-MS can be also used for a single particle analysis as reported by Scadding et al. They adopted the LA-ICP-TOF-MS for a fast forensic analysis of micro debris [11]. Admon et al. reported on the relocation technology of swiped particles during an isotope analysis of single microparticles by using SEM-to-SEM and SEM-to-SIMS experiments [12].

Recently, a direct analysis of elements as well as isotopes by using a laser ionization (or laser ablation) has been recognized as one of the convenient detection technologies for isotope

* Corresponding author. Tel.: +82 42 868 8226; fax: +82 42 868 8230.
E-mail address: sks@kaeri.re.kr (K. Song).

analysis of solid samples [13–16]. The laser ionization mass spectrometry (LIMS) requires only one laser source without a frequency tunability with no sample pretreatment. By adopting an intense laser light, an atomization as well as an ionization of target samples can be done in one step without additional ionization methods. Therefore the instrumentation for LIMS is rather compact when compared to the other methods described above. A direct LIMS can also be utilized for an isotope analysis of microparticles if enough ions are generated by the ablation process. When the LIMS is applied for an isotope analysis of microparticles, it is important to sustain the particle samples in the ablation region by controlling the parameters related to the laser in order to obtain multiple measurements of the mass spectra. In the present study, we present the experimental results of an isotope analysis for metal microparticles of various sizes by adopting a direct non-resonant LIMS with a slightly defocused laser beam. The slightly defocusing of the laser beam provided a longer duration for an isotope analysis with a single particle. Isotope abundance of the small sized particles ($<10\ \mu\text{m}$) and large sized particles ($50\text{--}75\ \mu\text{m}$) were measured and the effect of the particle size on the mass resolution was also discussed.

2. Experimental

The characteristics of a laser-induced plasma depend on a variety of experimental parameters such as wavelength, energy, pulse width of the ablating laser, and the characteristics of target samples. Among the available laser sources, the 2nd harmonic (532 nm) and 3rd harmonic (355 nm) of the Nd:YAG laser are popular choices as ablation wavelengths. In this study the 2nd harmonic of the Nd:YAG laser (Spectra Physics GCR-150), 532 nm, operated at a repetition rate of 10 Hz with a pulse width of 8 ns was used for the laser ablation of particle samples. Laser light was slightly defocused at the target particle with a beam size of $0.01\ \text{cm}^2$ ($1.7\ \text{mm} \times 0.8\ \text{mm}$) by adjusting the position of a focusing lens ($f=25\ \text{cm}$). The sample was attached to a repelling electrode in an ion source assembly of a reflectron type time-of-flight mass spectrometer (RMJordan Co. model D-850) and $\sim 2960\ \text{V}$ of dc high voltage was applied to a sample electrode in order to repel the generated ions in the direction of ion reflector. Two additional electrodes, one with 610 V and the other with a ground voltage, accelerated the generated ions in the direction of an ion mirror. Four deflection electrodes were also installed for the adjustment of the ion path in the x - and y -directions. The reflected ions were detected by using a dual micro channel plate. The detected ion signals were amplified by a preamplifier (SRS 240) and were measured by a digital oscilloscope (Lecroy model LT364). The TOF-MS was operated at a pressure of 1×10^{-7} Torr by a turbo molecular pump (Acatel ATP 900) backed up by a mechanical pump (Acatel 2033). The signal output from the preamplifier was averaged from more than 200 times of sweeps. The detailed experimental setup of the LIMS is shown in Fig. 1.

Particle samples were purchased from Aldrich and Newmet and used without further treatment. The adopted particle samples were Pb (99.999%), Ni (99.9%), Gd_2O_3 (99.99+%), and Zn (99.999%). Target samples for a laser ablation were prepared by

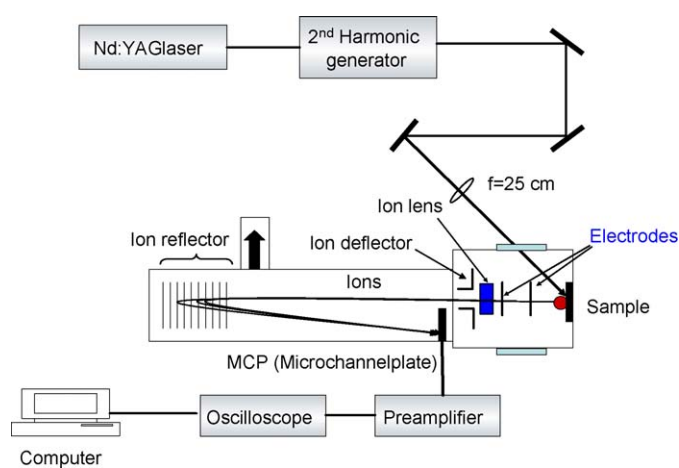


Fig. 1. A schematic diagram of the laser ionization mass spectrometry constructed for isotope analysis of micro-particles.

using a Collodion solution to fix a particle or several particles onto a metal sheet. Gadolinium oxide particles were loaded onto a zirconium sheet, while other particle samples were loaded onto a tantalum sheet. The sizes of sample particles were 75, 50, 10, and $<10\ \mu\text{m}$, for Pb, Zn, Ni and Gd_2O_3 , respectively. For Pb and Zn, the particles were mounted by using a brush needle which was made by cutting one hair of a painting brush at an angle. For smaller sized microparticles such as Ni and Gd_2O_3 , a dilution with distilled water was necessary in order to minimize the number of particles loaded in one step. Nevertheless several particles were loaded in one sampling spot for Gd_2O_3 and Ni particles. Fig. 2 shows the prepared sample plate and a magnified view of loaded particles. Since the sample particle was located inside the Collodion, the laser beam ablated the Collodion solution as well as particles. But the Collodion did not influence either in the generation of sample ions or the process of obtaining the mass spectrum of the target particle.

3. Results and discussion

In the previous report on the laser ionization mass spectroscopic studies for metal samples, we arranged the laser beam not to focus so tightly onto the sample surface in order to decrease the sample consumption [13,14]. In addition, an optimization of the density of the laser-induced plasma provided a high mass resolution by minimizing a space charge effect. The same approach was adopted in the present study. By adopting a slightly defocused laser beam for the ablation process, a sample particle lasted for enough to obtain multiple measurements of mass spectra for single microparticle with the laser source operated at 10 Hz. Adoption of a larger sized laser beam in the laser ablation process made an alignment of the laser beam onto the samples particle easy while it also created more chance for an ablation of the adjacently mounted particles. Therefore the particle samples have to be spatially separated so as not to ablate more than one particle at a time if a single particle analysis is desired. Fig. 2(a) shows the Zn particles loaded onto the Ta sheet. Three particle samples were loaded onto one Ta sheet with some distance among samples. When the Zn particles were purchased from the

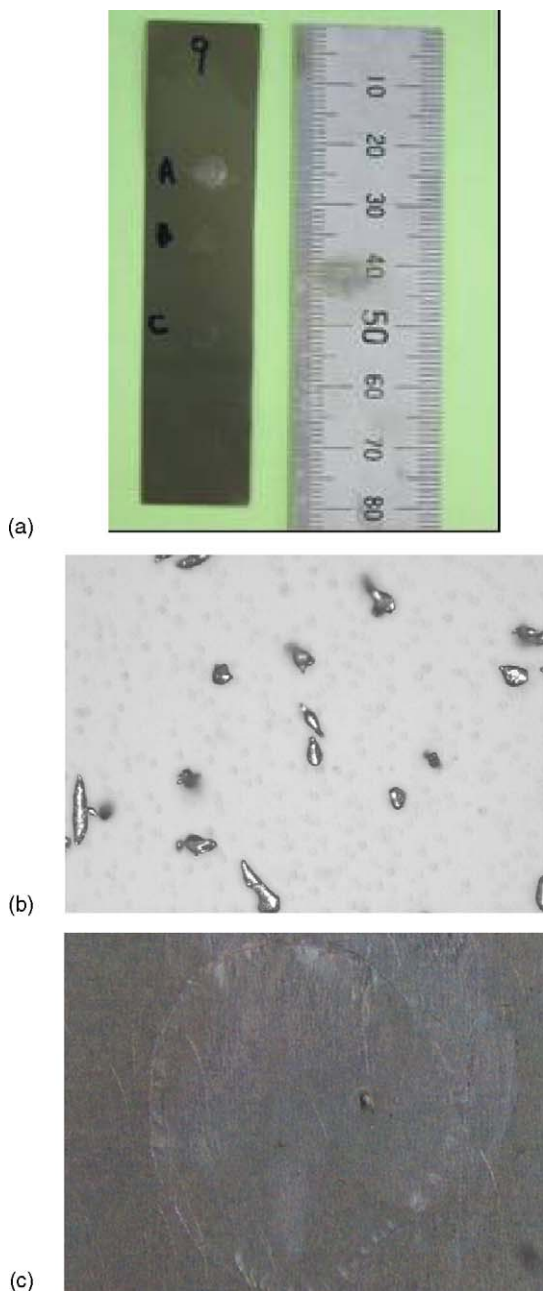


Fig. 2. Sample plate loaded with three Zn particles (a), various size of zinc particles (b), and loaded Zn particle after the laser ablation (c).

manufacturer, various sizes of particles were mixed as shown in Fig. 2(b). Therefore we selected a specific size of Zn particles by measuring the sizes of particles by using a microscope. The size of loaded Zn particle was approximately 50 μm . The picture of particle sample after a laser ablation is shown in Fig. 2(c). As can be seen in Fig. 2(c), the particle sample remained at the initially loaded position in spite of several measurements of mass spectra, while the Collodion was slightly damaged by the laser light. The white shade shown in this figure was generated due to the laser ablation of the Collodion. This figure clearly indicates that the present method for a laser ablation of single particle can hold particle sample for a long enough time while generating detectable amount of ions. Even smaller sized particles, such as

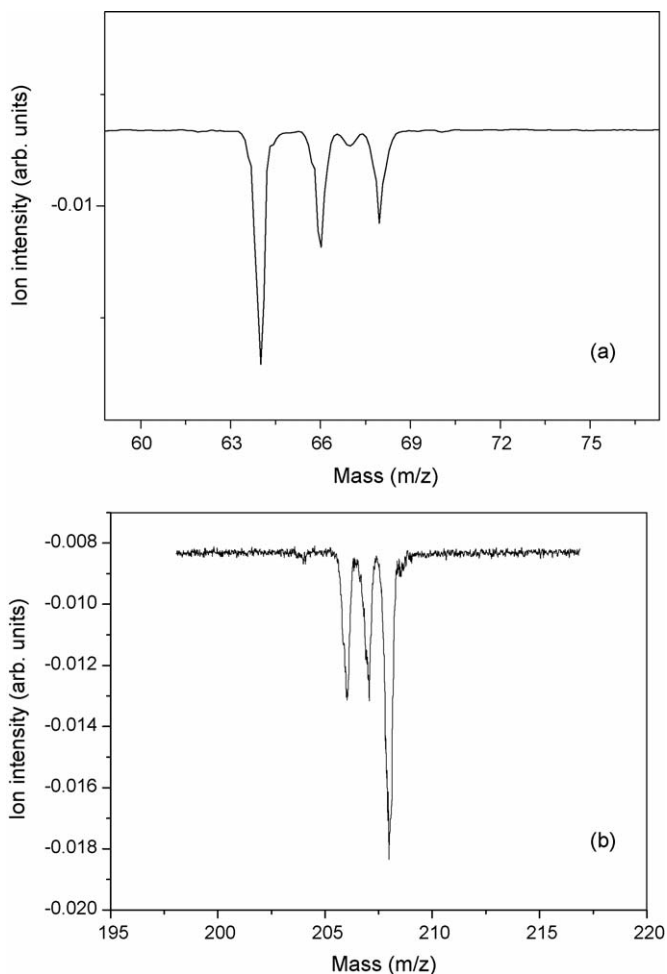


Fig. 3. Laser ionization mass spectrum of Zn (a) and Pb (b) particle loaded on the Ta plate. The power of ablation laser was 20 mW at 532 nm.

Ni and Gd_2O_3 , also showed ion signals for more than a few tens of minutes.

Fig. 3(a) shows the laser ionization mass spectrum for one of the Zn particles by using 532 nm laser as an ablation source. The laser power used for the ablation was 20 mW with focusing size of 0.01 cm^2 . Table 1 lists the isotopic ratio of Zn particles based on the measured mass spectra. More than ten measurements were undertaken to obtain the listed isotope abundance. The analyzed data for Zn isotopes agreed with a natural abundance within 10% except for isotope of $m/z = 70$. As can be seen from Table 1, most of isotopes shows very accurate abundances except for $m/z = 70$ if the standard deviations are being compared. The large error in the measurement of isotope abundance for $m/z = 70$ may be due to the effect of collisions inside the laser-induced plasma

Table 1
Result of isotope ratio measurement for Zn micro-particles

	Zn particle 1				
	$m/z = 64$	$m/z = 66$	$m/z = 68$	$m/z = 69$	$m/z = 70$
Natural abundance (%)	48.6	27.9	4.1	18.8	0.6
Averaged abundance (%)	50.86	26.69	3.82	17.99	0.63
Standard deviation (%)	1.2045	0.0851	0.3722	0.7050	0.15

Table 2
Result of isotope ratio measurement for Pb micro-particles

	$m/z=204$	$m/z=206$	$m/z=207$	$m/z=208$
Natural abundance (%)	1.4	24.1	22.1	52.4
Averaged abundance (%)	2.18	25.68	21.32	50.82
Standard deviation (%)	0.6305	0.9478	1.1227	0.5305

which may result in the deterioration of isotope ratios between highly abundant isotope and less abundant isotope. In addition small deterioration of the ion signal intensity for a less abundant isotope may be amplified while calculating isotope ratio when compared to the highly abundant isotopes. Fig. 3(b) is a laser ablation mass spectrum of the single particle of Pb by using 20 mW of an average laser power at 532 nm. The sizes of Pb particles were approximately 75 μm . Four stable isotopes of Pb, ^{204}Pb , ^{206}Pb , ^{207}Pb and ^{208}Pb were detected with a reasonable mass resolution of 600. The result of isotope analysis showed that an measured isotope ratio agrees to the natural abundance to within 5% of an error as shown in Table 2 except for the isotope of $m/z=204$.

The laser ablation technique was also applied for an isotope analysis of smaller sized microparticles. The size of Gd_2O_3 and Ni particles were measured as less than 10 μm . The lack of sample handling technology prevented the loading of a single particle with a 10 μm size. Therefore, several particles were loaded onto a metal sheet with Collodion, however microparticles might be ablated at the same time in a different position of the target plate, which might result in a poor mass resolution. The measured laser ionization mass spectrum of Gd_2O_3 particle is shown in Fig. 4(a). The mass resolution was identified to be 590 which was similar to the Pb or the Zn cases. The similar mass resolution between the large particles and the small particles may be due to the size of laser beam which is larger than the particle size. A large size of laser beam at the ablation spot means the size of the ablated plume will be similar even when the particle size is large or small as long as they are smaller than laser beam size. Therefore, the adoption of a slightly defocused laser beam for a particle ablation provided more advantage than that was expected. The Gd has seven stable isotopes ($m/z=152, 154, 155, 156, 157, 158, 160$), and the figure shows all seven isotopes as well as isotopes of oxide from, GdO . In general, ion signals generated from the oxide forms shows higher intensity when compared to the metal ions for the lanthanide elements at a low power of the ablation laser. The intensity ratio between Gd and GdO can be changed depending on the laser power or duration of the laser ablation. In the present study, the isotope ratio among GdO isotopes was used for an estimation of an

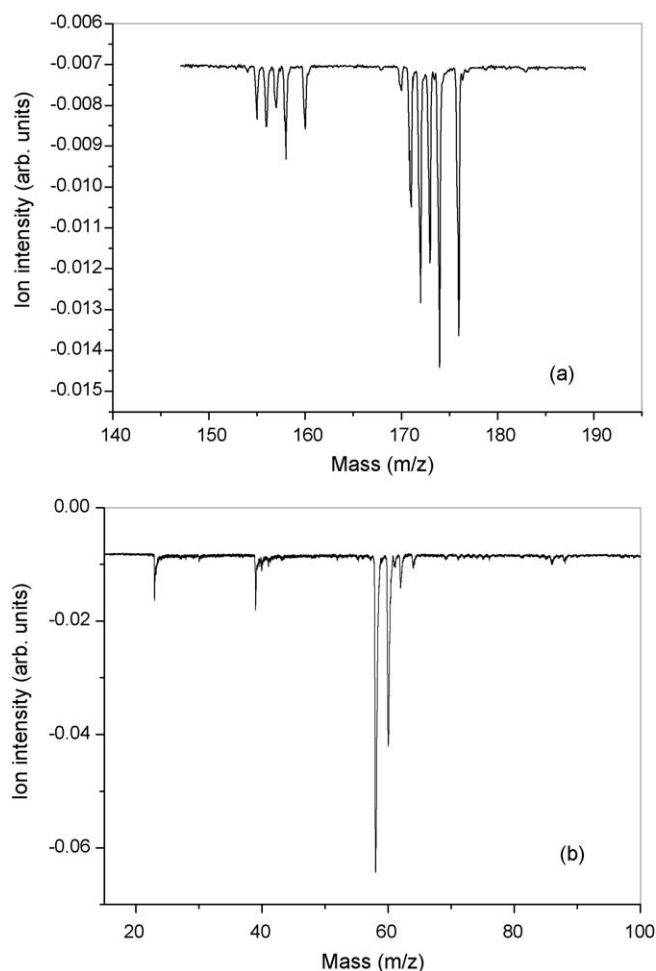


Fig. 4. Laser ionization mass spectrum of Gd (a) and Ni (b) microparticle.

abundance as shown in Table 3. The calculated abundance for the other isotopes based on the measured mass spectra agreed to within 5% of the natural abundance except for $m/z=168$. The laser ablation mass spectrum of Ni is shown in Fig. 4(b). Nickel has four isotopes ($m/z=58, 60, 61, 62, 64$) and they are clearly shown in Fig. 4(b). The isotope abundances were calculated as 65.96%, 26.44%, 1.40%, 3.56%, 2.64% for isotopes of $m/z=58, 60, 61, 62, 64$, respectively, as shown in Table 4. Isotope abundance of $m/z=64$ isotope was calculated much larger than the natural abundance, 0.92%. This is due to an overlap of the ion signals from the major isotope of TiO ($m/z=64$) which might be contained in the tantalum sheet as a minor impurity. Ion signals for $m/z=64$ contained isotopes of Ni as well as TiO . Therefore it was difficult to accurately calculate the isotope abundances for each of the Ni isotopes. The calculated isotope abundance

Table 3
Result of isotope ratio measurement for GdO micro-particles

	$m/z=168$	$m/z=170$	$m/z=171$	$m/z=172$	$m/z=173$	$m/z=174$	$m/z=176$
Natural abundance (%)	0.2	2.18	14.8	20.47	15.65	24.84	21.86
Averaged abundance (%)	0.27	2.18	15.22	20.10	16.63	23.79	21.81
Standard deviation (%)	0.0008	0.4536	0.3502	1.0848	0.4484	1.2226	0.7300

Table 4
Result of isotope ratio measurement for Ni micro-particles

	$m/z=58$	$m/z=60$	$m/z=61$	$m/z=62$	$m/z=64$
Natural abundance (%)	68.08	26.22	1.14	3.63	0.93
Averaged abundance (%)	65.96	26.44	1.40	3.56	2.64
Standard deviation (%)	1.56	1.61	0.14	0.13	1.03

is listed in Table 4. A more accurate determination of the isotope abundance with avoiding an overlap of ion signals from different elements can be achieved by a resonant laser ablation technique which can selectively ionize only Ni particles with resonant enhancement. This study is in progress.

4. Conclusion

We have demonstrated that a fast isotope analysis of micro-particles can be achieved by adopting a laser-ionization mass spectrometry. An optimization of focusing size of ablation laser beam on the target particles provided a long-time measurement which resulted in an improved accuracy by averaging several measurements. This technique requires a much simpler instrumentation when compared to SIMS or SNMS for a microparticle analysis. The measured isotope abundance of Zn, GdO, and Pb particles except for minor isotopes agrees within 5–10% of the natural abundance. For the Ni particles, the ion signal from TiO contained in the Ta sheet prevented an accurate measurement of the isotope abundance. This technique may be applied for an isotope analysis of swipe samples, if a further improvement of the accuracy and precision of the measured isotope ratio can be achieved.

Acknowledgement

This study was supported by the Long-term Nuclear R&D Project from MOST of Korea.

References

- [1] R. Zimmermann, T. Ferge, M. Galli, R. Karlsson, *Rapid Commun. Mass Spectrom.* 17 (2003) 851.
- [2] M.A. Stowers, A.L. van Wuijckhuijse, J.C.M. Marijnissen, B. Scarlett, B.L.M. van Baar, *Rapid Commun. Mass Spectrom.* 14 (2000) 829.
- [3] C.A. Noble, K.A. Prather, *Mass Spectrom. Rev.* 19 (2000) 248.
- [4] B. Oktem, M.P. Tolocka, M. Johnston, *Anal. Chem.* 76 (2004) 253.
- [5] G. Tamborini, M. Betti, *Mikrochim. Acta* 132 (2000) 411.
- [6] G. Tamborini, M. Betti, V. Forcina, T. Hiernaut, B. Giovannone, L. Koch, *Spectrochim. Acta Part B* 53 (1998) 1289.
- [7] G. Tamborini, M. Wallenius, O. Bildstein, L. Pajo, M. Betti, *Mikrochim. Acta* 139 (2002) 185.
- [8] N. Edermann, M. Betti, F. Kollmer, A. Benninghoven, C. Gruning, V. Philipson, P. Lievens, R.E. Silverans, E. Vandeweert, *Anal. Chem.* 75 (2003) 3175.
- [9] Y.J. Park, K. Song, H.Y. Pyo, M.H. Lee, K.Y. Jee, W.H. Kim, *Nucl. Instrum. Meth. Phys. Res. A* 557 (2006) 657.
- [10] O. Stzer, M. Betti, J. van Geel, N. Edermann, J. Kratz, R. Schenkel, N. Trautmann, *Nucl. Instrum. Meth. Phys. Res. A* 525 (2004) 582.
- [11] C.J. Scadding, R.J. Walting, A.G. Thomas, *Talanta* 67 (2005) 414.
- [12] U. Admon, D. Donohue, H. Aigner, G. Tamborini, O. Bildstein, M. Betti, *Microsc. Microanal.* 11 (2005) 354.
- [13] K. Song, H. Cha, D.H. Kim, K.H. Min, *Bull. Kor. Chem. Soc.* 25 (2004) 101.
- [14] K. Song, D.H. Kim, H. Cha, Y.K. Kim, E.C. Jung, I. Choi, H.S. Yoo, S.W. Oh, *Microchem. J.* 76 (2004) 95.
- [15] C.G. Gill, A.W. Garrett, P.H. Hemberger, N.S. Nogar, *Spectrochim. Acta Part B* 51 (1996) 851.
- [16] F. Costache, M. Ratzke, D. Wolfframm, J. Reif, *Appl. Surf. Sci.* 247 (2005) 249.